RESEARCH ARTICLE

Human Mutation

OFFICIAL JOURNAL
HGVS
HUMAN GENOME VARIATION SOCIETY
www.hgvs.org

Dilated Cardiomyopathy-Associated *BAG3* Mutations Impair Z-Disc Assembly and Enhance Sensitivity to Apoptosis in Cardiomyocytes

Takuro Arimura,[1] Taisuke Ishikawa,[1] Shinichi Nunoda,[2] Sachio Kawai,[3] and Akinori Kimura[1,4]*

[1]*Department of Molecular Pathogenesis, Medical Research Institute, Tokyo Medical and Dental University, Tokyo, Japan;* [2]*Department of Medicine, Tokyo Women's Medical University Medical Center East, Tokyo, Japan;* [3]*Department of Sports Medicine, Juntendo University Graduate School of Health and Sports Science, Tokyo, Japan;* [4]*Laboratory of Genome Diversity, School of Biomedical Science, Tokyo Medical and Dental University, Tokyo, Japan*

Communicated by Mark H. Paalman

Received 4 May 2011; accepted revised manuscript 24 August 2011.
Published online 6 September 2011 in Wiley Online Library (www.wiley.com/humanmutation).DOI: 10.1002/humu.21603

ABSTRACT: Dilated cardiomyopathy (DCM) is characterized by dilation of left ventricular cavity with systolic dysfunction. Clinical symptom of DCM is heart failure, often associated with cardiac sudden death. About 20–35% of DCM patients have apparent family histories and it has been revealed that mutations in genes for sarcomere proteins cause DCM. However, the disease-causing mutations can be found only in about 17% of Japanese patients with familial DCM. Bcl-2-associated athanogene 3 (BAG3) is a co-chaperone protein with antiapoptotic function, which localizes at Z-disc in the striated muscles. Recently, *BAG3* gene mutations in DCM patients were reported, but the functional abnormalities caused by the mutations are not fully unraveled. In this study, we analyzed 72 Japanese familial DCM patients for mutations in *BAG3* and found two mutations, p.Arg218Trp and p.Leu462Pro, in two cases of adult-onset DCM without skeletal myopathy, which were absent from 400 control subjects. Functional studies at the cellular level revealed that the DCM-associated *BAG3* mutations impaired the Z-disc assembly and increased the sensitivities to stress-induced apoptosis. These observations suggested that *BAG3* mutations present in 2.8% of Japanese familial DCM patients caused DCM possibly by interfering with Z-disc assembly and inducing apoptotic cell death under the metabolic stress.
Hum Mutat 32:1481–1491, 2011. © 2011 Wiley Periodicals, Inc.

KEY WORDS: dilated cardiomyopathy; DCM; *BAG3*

Introduction

Dilated cardiomyopathy (DCM) is a primary heart muscle disorder caused by functional abnormalities in the cardiomyocytes, which is characterized by ventricular chamber dilation and diminished cardiac contractility. DCM is a major cause of chronic heart failure and the most common indication for cardiac transplantation [Maron et al., 2006]. Various etiologies including gene mutations, viral infections, toxins such as alcohol, mitochondrial abnormalities, and metabolic disorders cause DCM [Maron et al., 2006]. Because 20 to 35% of DCM patients have family histories mostly consistent with autosomal dominant inheritance, linkage studies in multiplex families and/or candidate gene approaches have been taken to identify the disease genes and it has been revealed that DCM can be caused by various genetic abnormalities [Kimura, 2010]. The majority of genetic causes are heterozygous mutations in genes for sarcomere proteins including contractile elements, sarcolemma elements, Z-disc elements, and Z-I region components, which play key roles in the generation and/or transmission of contractile force. On the other hand, it has recently been demonstrated by extensive whole-genome analyses that sequence variations in the gene for Bcl-2-associated athanogene 3 (*BAG3*; MIM# 603883) were associated with DCM (CMD1HH; MIM# 613881) [Norton et al., 2011; Villard et al., 2011], although molecular mechanisms of DCM caused by the *BAG3* mutations are not fully unraveled.

BAG3 is a member of antiapoptotic BAG protein family. BAG3 protein binds heat shock protein 70 (Hsp70; MIM# 140550) within the C-terminal BAG domain, which is an evolutionary conserved domain among the BAG family, and serves as a co-chaperone factor controlling the chaperone activity of Hsp70 [Takayama et al., 1999]. It was reported that *BAG3* prominently expressed in the striated muscle and localized at the Z-discs [Homma et al., 2006]. In addition, *Bag3* knockout mice displayed degeneration of muscle fibers with apoptotic nuclei in the striated muscles, resulting in a severe form of skeletal myopathy and cardiomyopathy, which lead to a hypothesis that BAG3 protein might play a role as a Z-disc signaling molecule [Homma et al., 2006]. In accordance with the hypothesis, apart from the association with DCM described above [Norton et al., 2011; Villard et al., 2011], a heterozygous Pro209Leu mutation was found in patients with myofibrillar myopathy (MFM) accompanied by cardiomyopathy (MFM6; MIM# 612954) [Lee et al., 2011; Odgerel et al., 2010; Selcen et al., 2009]. Moreover, it was demonstrated that knockdown of *bag3* in a zebrafish model developed heart failure resembling to human DCM [Norton et al., 2011].

*Correspondence to: Akinori Kimura, Department of Molecular Pathogenesis, Medical Research Institute, Tokyo Medical and Dental University, 1-5-45 Bunkyo-Ku, Tokyo 113-8510, Japan. E-mail: akitis@mri.tmd.ac.jp

Contract grant sponsors: Ministry of Education, Culture, Sports, Science and technology, Japan; Ministry of Health, Labor and Welfare, Japan; Japan Society for the Promotion of Science: Basic Scientific Cooperation Program between Japan and Korea; Association Française contre les Myopathies (AFM); Institute of Life Science; Tokyo Medical and Dental University.

We report here two heterozygous *BAG3* gene mutations, identified in Japanese patients with familial DCM, which cause abnormal Z-disc assembly and increase the sensitivity to apoptosis in cultured cardiomyocytes. This is the first report demonstrating that the stress-induced apoptotic cell death accompanied by abnormal sarcomerogenesis is associated with DCM.

Materials and Methods

Subjects

A total of 72 genetically unrelated Japanese patients with DCM were included in this study. Each patient had an apparent family history (at least one patient among the first-degree family relatives). The patients were diagnosed based on medical history, physical examination, 12-lead electrocardiogram, echocardiography, and other special tests if necessary. The diagnostic criteria for DCM were described previously [Hayashi et al., 2004] and the patients who manifested with apparent skeletal muscle involvement were excluded from the study. The patients had been analyzed for mutations in 22 known cardiomyopathy-associated genes including genes for titin/connectin (*TTN*), desmin (*DES*), αB-crystallin (*CRYAB*), ZASP/Cypher (*LDB3*), and four-and-half LIM protein 2 (*FHL2*) [Kimura, 2010], and no mutation was found in any of them. Four hundred Japanese healthy individuals served as controls. Blood samples were obtained from each subject after given informed consent. The protocol for research was approved by the Ethics Review Committee of Medical Research Institute, Tokyo Medical and Dental University, Tokyo, Japan.

Mutational Analysis

Genomic deoxyribonucleic acids (DNAs) extracted from peripheral blood of subjects were used to amplify protein-coding exons of *BAG3* (GenBank Accession No. NM_004281.3) by polymerase chain reaction (PCR) in exon-by-exon manner using primer pairs; 5′-CGAGGAGGCTATTTCCAGAC-3′ and 5′-TGCCGTCGAGGTGGCGCCACCGACC-3′ for exon 1, 5′-AGTGTTTCCTCTGCCAGGAG-3′ and 5′-TGGGAAGCACAGCGGCTTGCTC-3′ for exon 2, 5′-CAAGCCAGGGGAGTCATTTG-3′ and 5′-GACATACCACCATAACCAGTC-3′ for exon 3, 5′-CAATTTCTGTGACTTTCAGTCAG-3′ and 5′-GTCAGTCTTCTTGCCTTCAAAG-3′ for the 5′-side half of exon 4, and 5′-ATCCAGGAGTGCTGAAAGTG-3′ and 5′-AAGTCTCTGAAATGCATGCAAC-3′ for the 3′-side half of exon 4. The PCR condition was composed of a denaturing step of 95°C for 2 min, 30 cycles of 95°C for 30 sec, 56°C for 30 sec, and 72°C for 30 sec, followed by an additional extension step of 72°C for 2 min. The PCR products were analyzed by direct sequencing on both strands using Big Dye Terminator chemistry (version 3.1) and ABI3100 DNA Analyzer (Applied Biosystems, CA).

Amino Acid Sequence Comparison of BAG3 from Various Species

Amino acid sequences of human BAG3 protein predicted from NM_004281.3 were aligned with those of rhesus monkey (XM_001104106), cattle (NM_001082471), rat (NM_001011936), mouse (NM_013863), chicken (XM_001233434), xenopus (BC043807), and zebrafish (BC078249).

Indirect Immunofluorescence Microscopy

Complementary DNA (cDNA) of human *BAG3* were obtained by reverse transcriptase PCR from total messenger ribonucleic acid of adult heart. A wild-type (WT) full-length *BAG3* cDNA fragment spanned from bp307 to bp2034 of NM_004281.3 (corresponding to aa1-aa576). Five equivalent mutant cDNA fragments carrying a C to T (MFM-associated Pro209Leu mutation) [Selcen et al., 2009], a C to T (DCM-associated Arg218Trp mutation), a C to T (nondisease-associated Arg258Trp polymorphism), or a T to C (DCM-associated Leu462Pro mutation) substitution were obtained by the primer-directed mutagenesis method. The cDNA fragments of *BAG3* were cloned into pEGFP-C1 vector (Clontech, CA) and they were sequenced to ensure that no errors were introduced.

All care and treatment of animals were in accordance with the guidelines for the Care and Use of Laboratory Animals published by the National Institute of Health (NIH Publication 85-23, revised 1985) and subjected to prior approval by the local animal protection authority. Neonatal rat cardiomyocytes (NRCs) from one-day-old Sprague-Dawley rats were prepared as described previously [Arimura et al., 2009]. NRCs (1×10^4 cells) were plated onto the Collagen Type I Cellware 8-Well Culture Slide (BD Biosciences, MA) in low-glucose DMEM supplemented with 0.01 mg/ml insulin (Sigma-Aldrich, MO), 10% fetal bovine serum (FBS), and 1% penicillin/streptomycin at 37°C with 5% CO_2 for 24 hr. Each pEGFP-based construct (0.3 μg) was transfected into the cells with 0.6 μl of TransFectin Lipid Reagent (Bio-Rad, CA), according to the manufacturer's instructions. Forty-eight hours after the transfection, the NRCs were washed with PBS and fixed for 15 min in 100% ethanol at −20°C. Transfected cells were incubated in blocking solution and stained by primary mouse anti-α-actinin (1:800, Sigma-Aldrich) or anti-desmin (1:200, Dako, Glostrup, Denmark), followed by secondary Alexa fluor 568 goat anti-mouse IgG_1 (1:500, Molecular Probes, OR).

C2C12 cells (8×10^3 cells), a mouse myoblast cell line, were plated onto the gelatin-coated Lab-Tek 2 well Chamber Slide (Nalgen Nunc International, NY) in DMEM supplemented with 20% FBS and 1% penicillin/streptomycin at 37°C with 5% CO_2 for 24 hr. The cells were transfected with each pEGFP-based construct (2 μg) in 4 μl of Turbofect in vitro Transfection Reagent (Fermentas Inc., ML) according to the manufacturer's instructions. Forty-eight hours after the transfection, the cells were cultured in differentiation medium (DMEM with 2% horse serum, 0.01 mg/ml insulin, and 1% penicillin/streptomycin) for 5 days. Differentiated myotubes were washed with PBS, fixed for 15 min in 100% ethanol at −20°C, incubated in blocking solution, and stained by primary mouse anti-MF20 (1:50, DSHB in University of Iowa, IA) monoclonal antibody (Ab), followed by secondary Alexa fluor 568 goat anti-mouse IgG (1:500, Molecular Probes).

All cells were mounted on a cover-glass using Mowiol 4-88 Reagent (Calbiochem, Darmstadt, Germany) with 4′6-diamidino-2-phenylindole (DAPI, Sigma-Aldrich), and images from at least 200 transfected cells were analyzed by using the LSM510 laser-scanning microscope (Carl Zeiss Microscopy, Jena, Germany).

Apoptosis Assay

For the apoptosis assay, 24 hr after the transfection with *BAG3* constructs, the NRCs were cultured under serum-deprived (FBS-free medium) condition for additional 24 hr, washed with PBS, fixed for 1 hr in 4% paraformaldehyde/PBS at room temperature, and permeabilized for 2 min in 0.1% Triton X-100/0.1%

sodium citrate on ice. Apoptosis was evaluated with the terminal deoxynucleotidyltransferase-mediated dUTP nick end-labeling (TUNEL) assay using in situ Cell Death Detection Kit, TMR red (Roche Diagnostics, Mannheim, Germany) according to the manufacturer's instructions.

Quantitative analysis of apoptosis was performed with the Cell Death Detection ELISA^{PLUS} kit (Roche Diagnostics) according to the manufacturer's instructions. H9c2 cells, a cell line derived from rat embryonic ventricular myocardial cells, were cultured in DMEM supplemented with 10% FBS and 1% penicillin/streptomycin at 37°C with 5% CO_2. The *BAG3* constructs were transfected into H9c2 cells using the TransFectin Lipid Reagent (Bio-Rad) according to the manufacturer's instructions, and transfectants were selected using Geneticin (Life Technologies Japan Ltd., Tokyo, Japan). After establishment of the stable H9c2 transfectants, 4×10^3 cells in each line were plated onto collagen type I-coated 96-well plates. Doxorubicin (1 μM; Sigma-Aldrich) was added to culture media and the cells were cultured for various intervals (24, 48, and 72 hr). Cells were lysed with 0.2 ml of the lysis buffer provided in the kit at room temperature for 30 min. Quantities of histone-associated DNA fragments (mono- and oligonucleosomes) were determined by an absorbance at 405 nm and a reference at 490 nm. Numerical data were arbitrarily expressed as means ± SEM. Statistical differences were analyzed using two-way analysis of variance and then evaluated using a Turkey adjustment for post hoc multiple comparison. A *P*-value of less than 0.05 was considered to be statistically significant.

Results

Identification of BAG3 Mutations in DCM

We searched for *BAG3* variations in 72 proband patients with familial DCM and eight distinct variations were identified (Fig. 1A). Among them, two synonymous substitutions, Pro334Pro (c.1002T>G in exon 4, rs3858339) and Val432Val (c.1296A>G in exon 4, rs196295), and three nonsynonymous variations, Arg258Trp (c.772C>T in exon 3, rs117671123), Asp300Asn (c.898G>A in exon 3, rs78439745), and Pro407Leu (c.1220C>T in exon 4, rs3858340), were known polymorphisms registered in the dbSNP database (http://www.ncbi.nlm.nih.gov/projects/SNP/). In addition, a nonsynonymous variation, Glu553Asp (c.1659A>T in exon 4) found in one patient, was considered to be a polymorphism, because it was found in heterozygous state in nine of the 400 control subjects, that is allele frequency was 0.011 in Japanese patients.

On the other hand, two missense mutations, Arg218Trp (c.652C>T in exon 3) and Leu462Pro (c.1385T>C in exon 4), identified in heterozygous state in two DCM patients (designated II-1 in Fig. 1B and C, respectively) were not observed in the 400 control subjects. A family study suggested a co-segregation of the Leu462Pro mutation with DCM, because the mutation was present in a possibly affected sister, but not present in her father and brother who did not suffer from DCM (Fig. 1C). Most of the *BAG3* sequence variations including polymorphisms were found at the residues that were evolutionary conserved from various species except for zebrafish (Fig. 1D).

Clinical parameters of the patients with *BAG3* mutations are shown in Table 1. The proband patients carrying Arg218Trp or Leu462Pro mutation developed DCM at age 73 or 34, respectively, suggesting that the mutations was associated with DCM of adult onset. It should be noted that a sister of patient carrying the Leu462Pro mutation did not manifest with overt DCM at age 27, but she showed a slight systolic dysfunction of heart. Electrocardiogram findings of the affected individuals demonstrated no primary conduction defect. Serum creatine kinase (CK) level was not increased in both cases with the Leu462Pro mutation. They did not show apparent sign of skeletal myopathy or neuropathy.

Abnormal Assembly of Z-Discs Caused by the DCM-Associated BAG3 Mutations in NRCs

To investigate a possible functional consequence of the *BAG3* mutations, we analyzed cellular distribution of BAG3 proteins by using green fluorescence protein (GFP) chimeras of *BAG3* transfected into NRCs. For this purpose, we constructed GFP-tagged BAG3 of WT and DCM-associated mutations, Arg218Trp and Leu462Pro. We also tested an MFM-associated mutation, Pro209Leu [Lee et al., 2011; Odgerel et al., 2010; Selcen et al., 2009], and a nondisease-related missense variant, Arg258Trp (Fig. 1A), which was found in one patient and 11 controls in this study. Control NRCs transfected with GFP-alone construct showed diffuse localization of GFP signals (data not shown). Western blot analyses showed that the expression of each GFP–BAG3 construct was similar at the protein level in the transfected cells, suggesting that the mutation did not affect the expression of GFP–BAG3 (data not shown). In the mature myofibrils where Z-discs were well organized, GFP-BAG3-WT was assembled in the striated pattern and co-localized with α-actinin and desmin, markers for the Z-disc (Figs. 2A–C and 3A–C, respectively). It was found that most (~90%) of NRCs did not show nuclear localization of GFP-BAG3-WT (Figs. 2A–C and 3A–C). GFP-BAG3-Pro209Leu and GFP-BAG3-Arg258Trp also showed striated pattern co-localized with α-actinin and desmin at the Z-discs and did not show the nuclear localization (Figs. 2D–F and 3D–F, and Figs. 2J–L and 3J–L, respectively). In clear contrast, striated distribution was not found for both GFP-BAG3-Arg218Trp (Figs. 2G–I and 3G–I) and GFP-BAG3-Leu462Pro (Figs. 2M–O and 3M–O) in about 90% of transfected NRCs. Of note was that the Z-disc assembly represented by localization of α-actinin and desmin was impaired in the NRCs transfected with GFP-BAG3-Arg218Trp or GFP-BAG3-Leu462Pro (Figs. 2H and 3H, or Figs. 2N and 3N, respectively). Quite interestingly, these mutant proteins displayed localization within the nuclei in approximately 80% of the transfected NRCs (Figs. 2G and 3G, or Figs. 2M and 3M, respectively). These data suggested that the DCM-associated mutations disturbed the assembly and integrity of Z-discs, along with the nuclear localization of BAG3 protein, while such abnormalities were not observed with the MFM-associated mutations.

Myotube Formation was Affected by the MFM-Associated BAG3 Mutation but Not by the DCM-Associated BAG3 Mutations in C2C12 Cells

The DCM patients carrying *BAG3* mutations in this study did not manifest with apparent skeletal muscle involvement, but some other *BAG3* mutations were reported in patients with MFM. There is a possibility that the DCM-associated mutations might affect the function of BAG3 protein in striated muscles differently from the MFM-associated mutation. To investigate whether the *BAG3* mutations would affect the skeletal muscle differentiation from myoblasts to myotubes, C2C12 myoblast cells were transfected with BAG3 constructs and differentiated into multinucleated myotubes by low-serum culture condition. After 5 days of differentiation, myosin heavy chain positive (recognized by MF20 Ab) myotubes could often be observed in this condition. Control cells transfected with GFP-alone construct (data not shown) and the

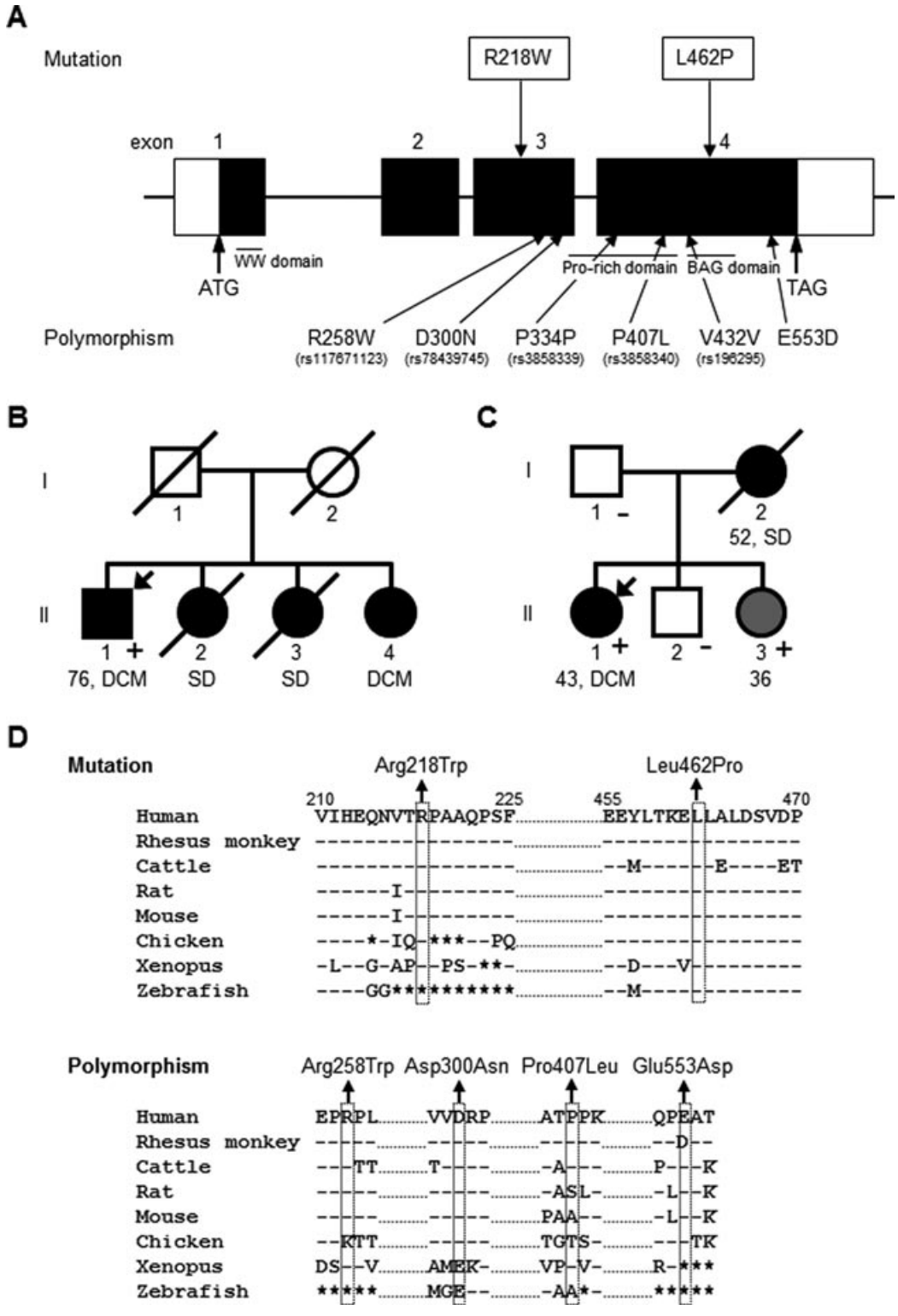

Figure 1. Mutational analysis of *BAG3* in dilated cardiomyopathy. A: Sequence variations found in this study are listed. Single-letter code is used to indicate the amino acid residue. DCM-associated mutations and polymorphisms are indicated above and below the schematic representation of *BAG3* gene, respectively. Known polymorphisms are indicated with reference single nucleotide polymorphism (rs) number in the parentheses. Solid boxes represent coding exons. B and C: Pedigrees of DCM families carrying the R218W mutation (B; CM 2019 family) or L462P mutation (C; CM 2053 family) are shown. Filled square and filled circle indicate affected male and female, respectively. Open square and open circle represent unaffected male and female with DCM, respectively. Arrows indicate the proband patients. Presence (+) or absence (–) of the mutations is noted for analyzed individuals. II-3 in (C), who is represented by a shadowed circle, showed a regional hypokinesia in posterior ventricular wall. SD, sudden death. D: Alignment of amino acid sequences of BAG3 proteins from various species around the DCM-associated mutations, Arg218Trp (R218W) and Leu462Pro (L462P), along with polymorphisms identified in the Japanese populations. Protein sequence of human BAG3 predicted from the nucleotide sequences was aligned with that of rhesus monkey, cattle, rat, mouse, chicken, xenopus, and zebrafish.

Table 1. Clinical Characteristics of Individuals Carrying BAG3 Mutations

ID	Mutation	Age at exam (years) and gender	Age at onset (years)	LVDd (mm)	LVDs (mm)	IVST (mm)	PWT (mm)	%FS	%EF	Other remarks
CM2019 family II-1	R218W	76, male	73	54	48	10	10	11	29	ECG; ectopic atrial rhythm,
CM2053 family II-1	L462P	41, female	34	59	47	6	6	20	40	ECG; premature ventricular contraction, CK = 66 IU/l
CM2053 family II-3	L462P	27, female	27	48	31	7	6	35	64	EchoCG; partial hypokinesia in posterior ventricular wall, CK = 62 IU/l

LVDd, left ventricular end-diastolic dimension; LVDs, left ventricular end-systolic dimension; IVST, interventricular septum thickness; PWT, posterior wall thickness; %FS, percent fractional shortening; %EF, percent ejection fraction; ECG, electrocardiogram; EchoCG, echocardiogram; CK, creatine kinase.

cells transected with GFP-BAG3-WT showed similar morphological differentiation, because about half (40 to 50%) of myotubes transfected with GFP-BAG3-WT were over trinucleation (Fig. 4A–C). Similarly, after 5 days of differentiation, numbers of myotubes with over trinucleation were about half in cells transfected with GFP-BAG3-Arg218Trp (Fig. 4G–I), GFP-BAG3-Arg258Trp (Fig. 4J–L), and GFP-BAG3-Leu462Pro (Fig. 4M–O). In clear contrast, most (∼90%) of myotubes transfected with GFP-BAG3-Pro209Leu were in binuclear state (Fig. 4D–F). These observations suggested that the MFM-associated mutation, Pro209Leu, might disturb the multinucleation during the differentiation into skeletal muscle myotubes. It should be noted that GFP-BAG3 proteins showed diffuse localization in the cytoplasm and did not show nuclear localization in the myotubes transfected with GFP-BAG3 constructs, even with the DCM-associated mutations (Fig. 4).

Altered Sensitivity to Apoptosis Caused by the DCM-Associated BAG3 Mutations

Because BAG3 is an antiapoptotic protein, we hypothesized that the *BAG3* mutations might render the cells susceptible to stress-induced apoptosis. To investigate the possible involvement of *BAG3* mutations in the abnormal regulation of cellular apoptosis, we first performed a TUNEL assay on NRCs transfected with GFP chimeras of *BAG3*. There was no difference in the frequency of TUNEL-positive cells among the nontransfected and transfected NRCs under the culture condition without serum starvation; less than 1% of NRCs were TUNEL positive. Under the serum-deprived condition for 24 hr, most (∼90%) of NRCs expressing GFP-BAG3-WT showed negative TUNEL staining (Fig. 5A–C). In contrast, about half of NRCs transfected with GFP-BAG3-Arg218Trp (Fig. 5G–I) or GFP-BAG3-Leu462Pro (Fig. 5M–O) demonstrated positive TUNEL staining with disorganized GFP signals under the serum deprivation for 24 hr, albeit most (∼90%) of NRCs transfected with GFP-BAG3-Pro209Leu (Fig. 5D–F) or GFP-BAG3-Arg258Trp (Fig. 5J–L) showed negative TUNEL staining with well-organized striated pattern of GFP signals. These observations indicate that the cardiomyopathy-associated *BAG3* mutations, but not the MFM-associated *BAG3* mutation or nondisease-related *BAG3* polymorphism, may increase the susceptibility to stress-induced apoptosis of NRCs.

To confirm the increased sensitivity to stress-induced apoptosis by the DCM-associated *BAG3* mutations by another method, we quantified apoptosis of H9c2 cells stably expressing GFP alone, GFP-BAG3-WT, or GFP chimera of each variant by the cell death ELISA assay. Stable transfected cell lines were treated with doxorubicin at the concentration of 1 μM for 24, 48, or 72 hr, and subjected to the assay. It was demonstrated that doxorubicin induced formation of oligonucleosomes in a time-dependent manner, and there was no significant difference among the nontransfected H9c2 cells and transfected cell lines expressing GFP only, GFP-BAG3-WT, GFP-BAG3-Pro209Leu, or GFP-BAG3-Arg258Trp (Fig. 6). On the other hand, significantly higher amounts of oligonucleosomes were observed in the stable transfectants expressing GFP-BAG3-Arg218Trp or GFP-BAG3-Leu462Pro than the transfectants expressing GFP-BAG3-WT, under the treatment by doxorubicin (Fig. 6). These observations further indicated that the DCM-associated *BAG3* mutations increased the sensitivities to apoptosis under the stressed condition.

Discussion

In the present study, we identified two DCM-associated mutations in a Z/I-band signaling protein, BAG3, which were not found in the controls and caused functional alterations. In addition, we found four other *BAG3* variations with amino acid replacements, but they were not considered to be associated with DCM, because they were present in the healthy individuals, even though evolutionary conserved residues were replaced. The DCM-associated mutations affected the Z-disc assembly of cardiomyocytes and increased the sensitivity to apoptosis under the metabolic stress. The latter functional change might be the reason for that the *BAG3* mutations were found in late-onset DCM. In other words, metabolic stresses to cardiomyocytes might be required to develop overt DCM in the subjects with the *BAG3* mutations found in this study.

We observed no functional alterations caused by the Arg258Trp variant in NRCs, a cardiomyocyte cell line H9c2, and a skeletal muscle cell line C2C12, suggesting that it was not a pathogenic mutation. Although the Arg258Trp mutation was recently reported in a Chinese patient with MFM, it was also found in the unaffected father of the patient and the patient carried another mutation Pro209Leu [Lee et al., 2011]. In this study, we demonstrated that the MFM-associated Pro209Leu mutation impaired the differentiation of skeletal muscle cell line C2C12, although it caused no functional alterations in the NRCs and in a cardiomyocyte cell line H9c2. The observations further suggested that the Arg258Trp variant was a simple polymorphism not associated with the diseases.

BAG3 is a co-chaperone protein and might not be directly involved in the muscle contractile function. Recent genetic studies have revealed that DCM is caused by the gene abnormalities not only in the cytoskeletal/contractile proteins, but also in the noncytoarchitectural molecules distributed in the Z/I-band region [Kimura, 2010]. We previously reported a DCM-associated Arg157His mutation in another chaperone protein, αB-crystallin, and this mutation did not show abnormal localization in the cytoplasm of NRC, whereas a myopathy-associated Arg120Gly mutation formed aggregated cytoplasmic depositions [Inagaki et al., 2006]. BAG3 and αB-crystallin bind with each other and both proteins serve to maintain protein homeostasis against the environmental stress [Hishiya

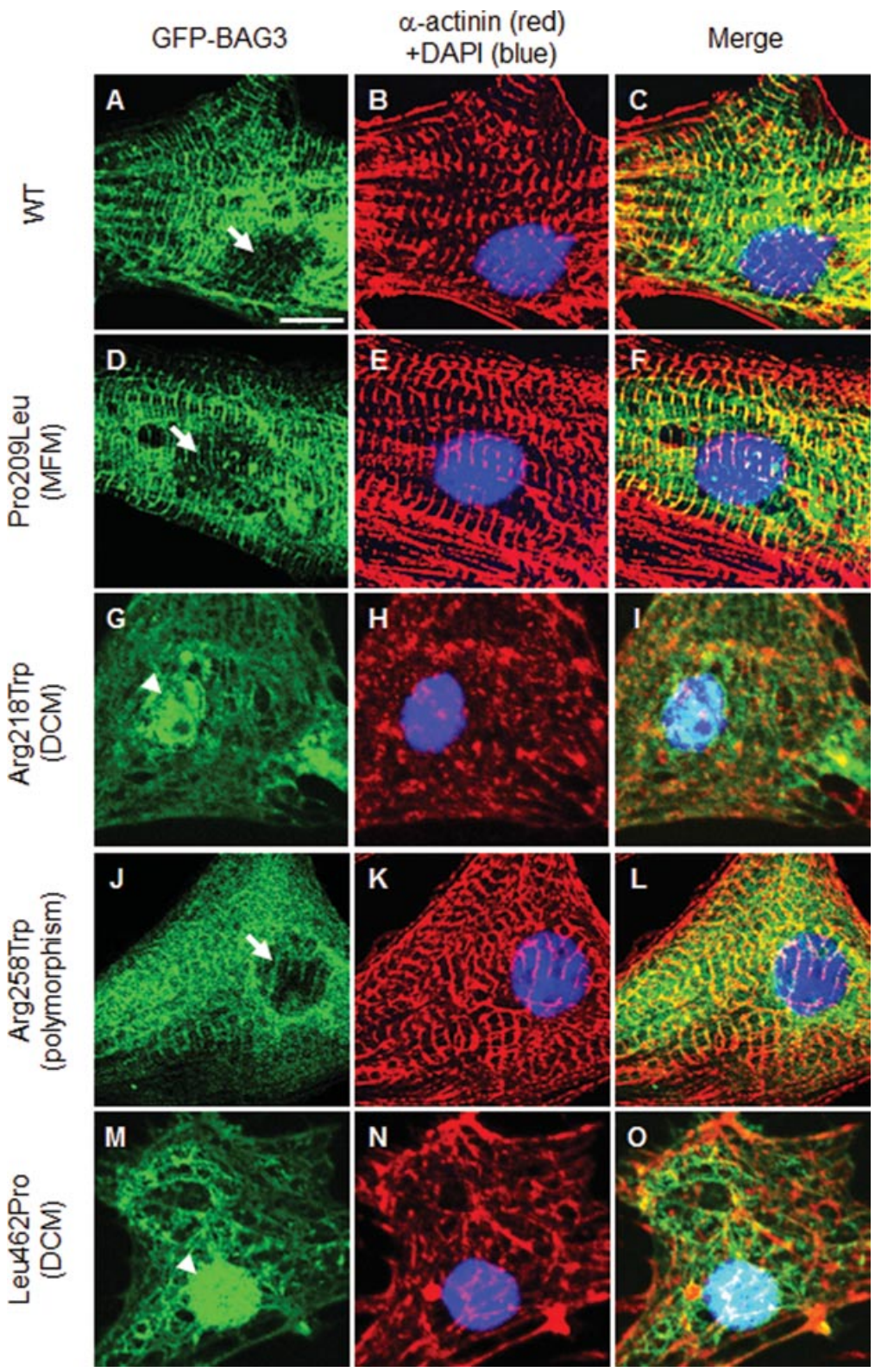

Figure 2. Distribution of α-actinin and transiently expressed GFP chimeras of *BAG3* in NRCs. NRCs transfected with GFP-tagged *BAG3* constructs for WT (A–C) or mutant (P209L, R218W, R258W, or L462P) (D–F, G–I, J–L, or M–O, respectively) were fixed 48 hr after the transfection, and stained with DAPI and anti-α-actinin antibody followed by secondary antibody (B, E, H, K, and N). Merged images are shown in C, F, I, L, and O. In the NRCs showing myofibrils with Z-discs, GFP-BAG3-WT is observed at the Z-discs and cytoplasm (A–C). GFP-tagged BAG3 proteins carrying the MFM-associated mutation, Pro209Leu, and nondisease-related variant, Arg258Trp, showed similar localization to that of WT (D–F and J–L, respectively). In contrast, GFP-tagged BAG3 proteins carrying the DCM-associated mutations, Arg218Trp and Leu462Pro, showed diffused localization that was associated with the disorganization of sarcomeric α-actinin (G–I and M–O). Arrows and arrowheads indicate the absence and presence, respectively, of GFP-BAG3 protein in nuclei. Scale bars = 10 μm.

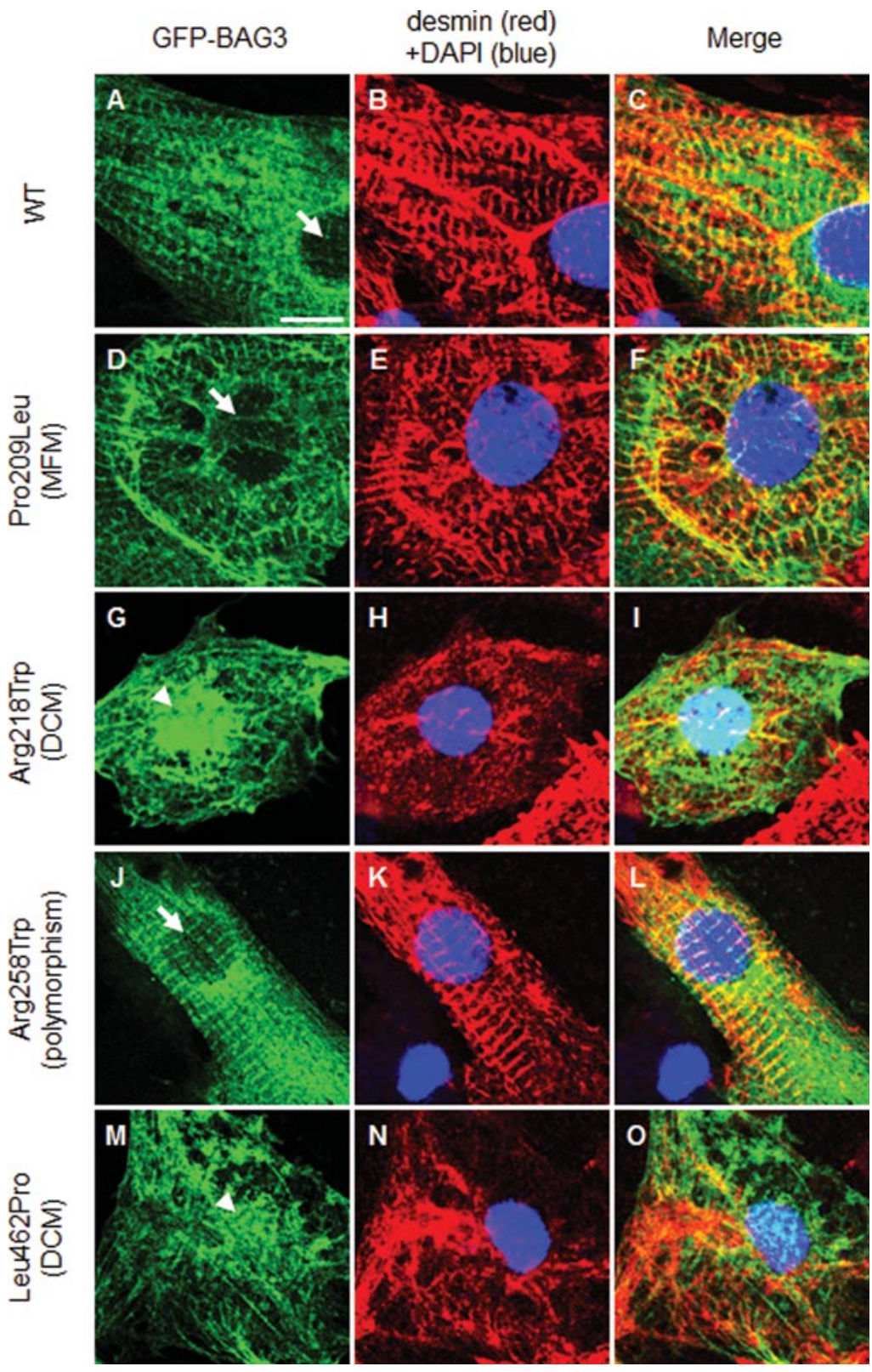

Figure 3. Distribution of desmin and transiently expressed GFP chimeras of BAG3 in NRCs. NRCs transfected with GFP-tagged BAG3 constructs for WT (A–C) or mutant (P209L, R218W, R258W, or L462P) (D–F, G–I, J–L, or M–O, respectively) were fixed 48 hr after the transfection, and stained with DAPI and anti-desmin antibody followed by secondary antibody (B, E, H, K, and N). Merged images are shown in C, F, I, L, and O. In the NRCs showing myofibrils with Z-discs, GFP-BAG3-WT is observed at the Z-discs and cytoplasm (A–C). GFP-tagged BAG3 proteins carrying the Pro209Leu and Arg258Trp, showed similar localization to that of WT (D–F and J–L, respectively). In contrast, GFP-tagged BAG3 proteins carrying the Arg218Trp and Leu462Pro, showed diffused localization that was associated with the disorganization of cytoskeletal desmin (G–I and M–O). Arrows and arrowheads indicate the absence and presence, respectively, of GFP-BAG3 in nuclei. Scale bars = 10 μm.

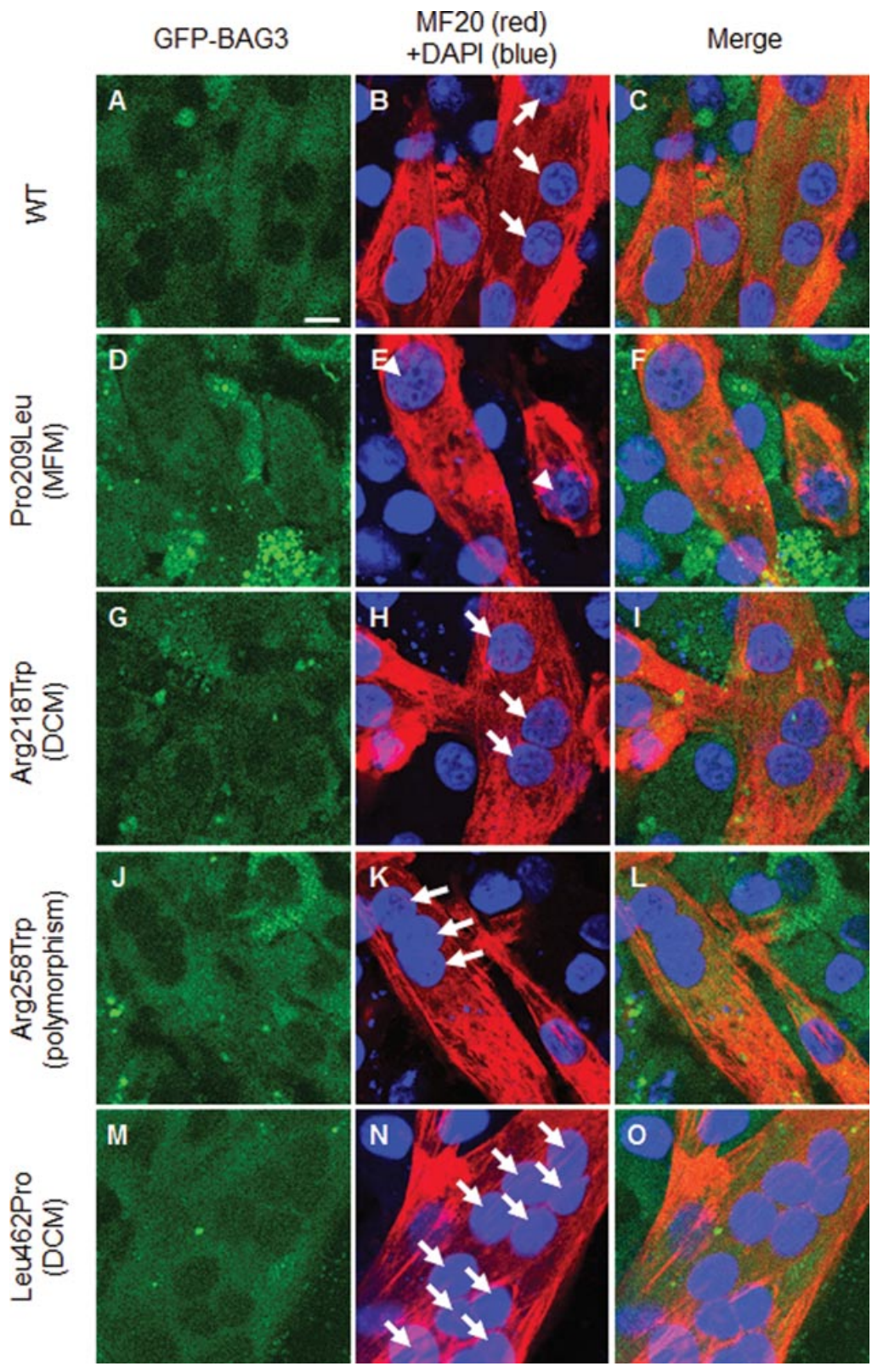

Figure 4. Differentiation of myoblasts into myotubes in C2C12 cells transiently expressed GFP chimeras of BAG3. C2C12 cells transfected with GFP-tagged BAG3 constructs for WT (A–C) or mutant (P209L, R218W, R258W, or L462P) (D–F, G–I, J–L, or M–O, respectively) were differentiated for 5 days in low-serum culture condition, and stained with DAPI and anti-MF20 antibody followed by secondary antibody (B, E, H, K, and N). Merged images are shown in C, F, I, L, and O. In the myotubes positively stained with MF20, GFP-BAG3 proteins were diffusely distributed in cytoplasm (A, D, G, I, and M). Trinucleations (arrows) were observed in the myotubes transfected with GFP- BAG3 WT, Arg218Trp, Arg258Trp, and Leu462Pro, but not in the myotubes transfected with GFP- BAG3 Pro209Leu (arrowheads). Scale bars = 10 μm. [Color figure can be viewed in the online issue, which is available at wiley.com/humanmutation.]

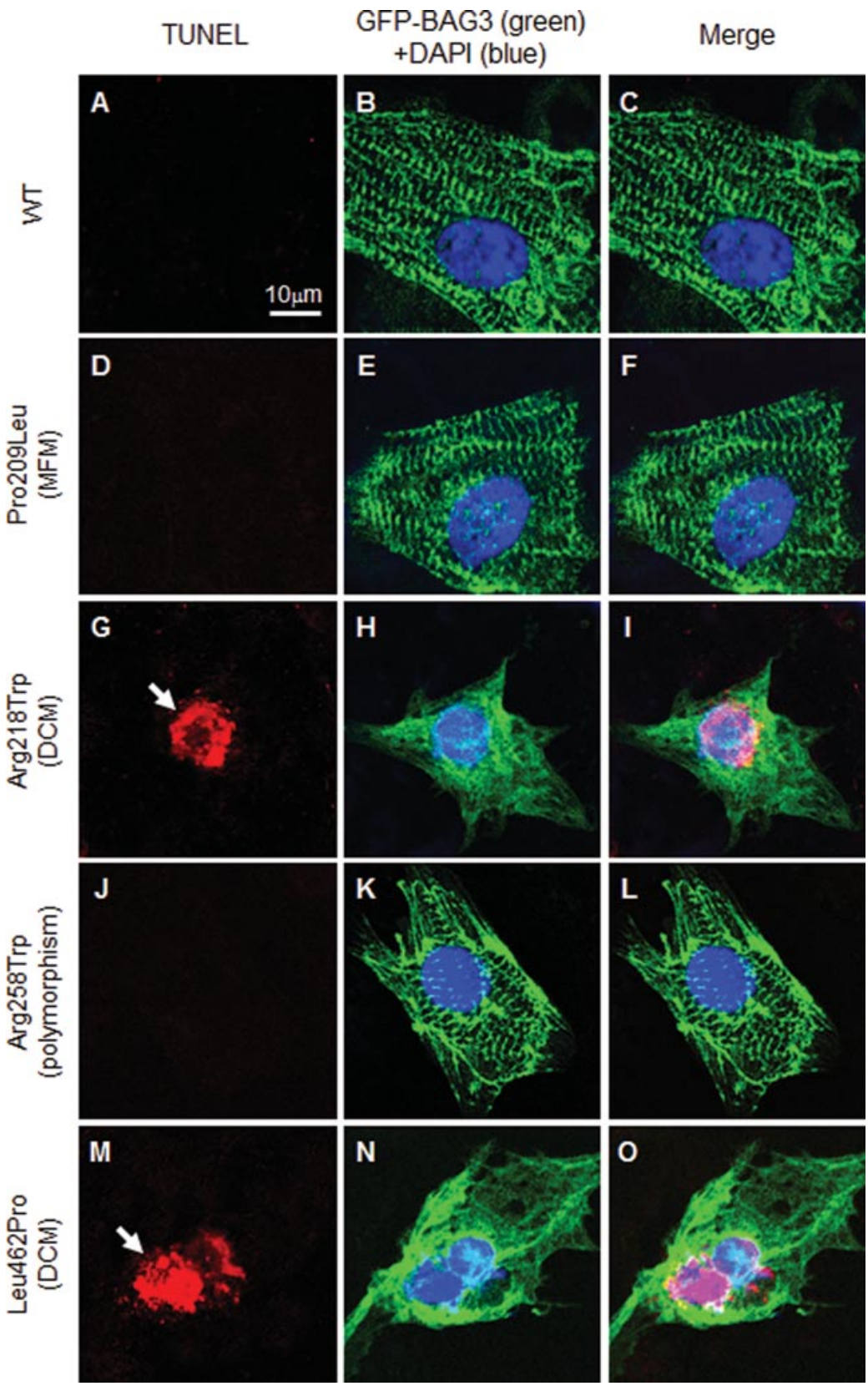

Figure 5. Apoptosis induced by serum deprivation in NRCs transfected with GFP-BAG3. NRCs were transfected with GFP chimeras of WT (A–C) or mutant (P209L, R218W, R258W, or L462P) (D–F, G–I, J–L, or M–O, respectively). The NRCs were cultured under FBS-free condition for additional 24 hr, fixed, subjected to the TUNEL assay, and stained with DAPI (B, E, H, K, and N). Merged images are shown in C, F, I, L, and O. Representative images of TUNEL assays are shown (A, D, G, J, and M). Arrows indicate apoptotic cells with positive TUNEL staining as visualized by red fluorescence; scale bars = 10 μm. [Color figure can be viewed in the online issue, which is available at wiley.com/humanmutation.]

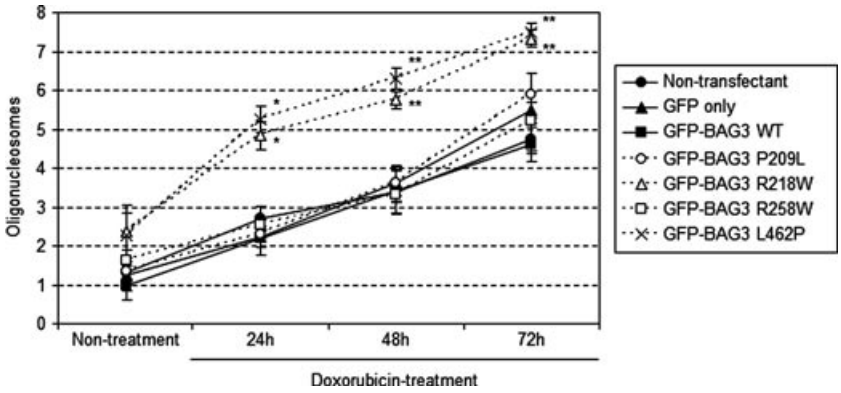

Figure 6. Quantitative analysis of apoptosis induced by doxorubicin in H9c2 cells stably expressing GFP-BAG3. H9c2 cells stably expressing each GFP chimera of *BAG3* in 96-well dishes were treated with 1 μM of doxorubicin for 24, 48, and 72 hr. Cell lysates were subjected to cell death ELISA assay. Amounts of mono- and oligonucleosomes were measured at 405 nm, and referenced by 490 nm. Data are arbitrarily expressed as means ± SEM ($n = 6$ for each case). * $P < 0.01$ versus WT; ** $P < 0.001$ versus WT.

et al., 2011]. In addition, they have crucial roles in protein folding, inhibition of protein aggregation, and degradation of misfolded proteins as chaperone-related proteins [Hishiya et al., 2011]. However, disrupted co-localization of BAG3 and α-actinin was observed for GFP-BAG3-Arg218Trp and GFP-BAG3-Leu462Pro without any cytoplasmic aggregation of mutant BAG3 proteins, indicating that the abnormal Z-disc assembly was directly associated with the *BAG3* mutations. It is worth noting that the functional alteration caused by the DCM-associated *BAG3* mutations was different from that by the DCM-associated αB-crystallin mutation, which was the decreased binding to titin N2-B region without disturbing the Z-disc assembly [Inagaki et al., 2006].

The mechanism of altered Z-disc assembly caused by the DCM-associated *BAG3* mutations is not clear, but a knockdown of *Bag3* in cardiomyocytes induced rapid myofibrillar degeneration and Z-disc disruption under the condition of mechanical stress [Hishiya et al., 2010], suggesting that *BAG3* might play a pivotal role in the Z-disc assembly during the myofibrillogenesis. In the transition from nascent to mature myofibrils, Z-disc precursors, Z-bodies, eventually fuse laterally to form Z-discs at the trunk of myocytes, which is accompanied by the induction of myofibrillar proteins, and this may stabilize the sarcomere structure required for muscle contraction. In this study, it was suggested that the DCM-associated mutations affected the assembly of sarcomere in NRCs. However, because we did not assessed the turnover and/or reorganization of the Z-discs, molecular mechanisms of disturbing the Z-disc organization during myofibrillogenesis should be further investigated in future studies.

The myofibrillar integrity under mechanical stress is maintained by the BAG3–Hsc70 interaction [Hishiya et al., 2010], and Hsc70 is a regulator of a chaperone-dependent E3 ligase CHIP [Murata et al., 2003; Pratt et al., 2010]. It was reported that CHIP-mediated degradation of p53 was involved in the protection against myocardial damage under ischemic condition [Naito et al., 2011]. These observations imply a possible link between the myofibrinogenesis and stress-induced apoptosis of cardiomyocytes. It is well known that serum deprivation and doxorubicin induce apoptosis of cultured cardiomyocytes including NRCs [Chao et al., 2005] and H9c2 cells [Chua et al., 2006], and we demonstrated that the DCM-associated *BAG3* mutations increased the sensitivity to apoptosis of the cardiomyocytes under the stressed conditions. Because BAG3 protein possess antiapoptotic function by enhancing the activity of bcl-2 [Lee et al., 1999], increased number of TUNEL-positive cells and oligonucleosomes in NRCs and H9c2 cells, respectively, expressing the DCM-associated *BAG* mutations might be due to the impaired function of BAG3 protein. Quite interestingly, we observed nuclear localization of GFP-BAG3-Arg218Trp and GFP-BAG3-Leu462Pro proteins in NRCs. Because the abnormal intranuclear accumulation was not observed in the NRCs transfected with GFP-BAG3-WT, GFP-BAG3-Pro209Leu, or GFP-BAG3-Arg258Trp, recruitment of BAG3 protein into nuclei may be a specific phenomenon caused by the DCM-associated mutations, which might be involved in the apoptosis of cardiomyocytes leading to DCM. Because the nuclear localization of mutant GFP-BAG3 proteins was observed in both apoptotic and nonapoptotic cells, we could not conclude whether the apoptosis was a direct consequence of the nuclear localization of mutant GFP-BAG3 proteins. Additional studies will be required to clarify the issue.

A number of skeletal muscle diseases and isolated DCM are caused by mutations in the same genes [Arimura et al., 2007]. The patients with muscular diseases often suffer from cardiac involvement, but most of the patients with isolated DCM do not manifest with the skeletal muscle phenotype. The etiological link between the inherited skeletal muscle diseases and hereditary DCM has raised a question as how the mutations in the genes/proteins expressed in both skeletal and cardiac muscles cause heart-specific phenotypes in the isolated DCM. The most probable explanation was that the phenotypic differences between the skeletal muscle disease and DCM might be due to that mutations in specific and/or different functional domains would affect specific functions. In this study, we found that the MFM-associated mutation, Pro209Leu, did not affect either the Z-disc assembly or the sensitivity to apoptosis. In clear contrast, the DCM-associated Arg218Trp mutations, which located near the Pro209Leu mutation, and the other DCM-associated Leu462Pro mutation caused abnormalities in both Z-disc assembly and sensitivity to apoptosis. It was reported that BAG3 protein with the Pro209Leu mutation was found predominantly in the abnormal form of small discrete granules in the COS-7 cells [Selcen et al., 2009], but such abnormality was not observed in NRCs, H9c2 cells, and C2C12 cells in this study. The reason why the Pro209Leu mutation did not show aggregations in the cardiomyocytes and skeletal muscle cell line is not clear, but the COS-7 cells are used for overexpression of genes from transfected constructs containing the replication origin of SV40, raising a possibility that the aggregation

was caused by the overexpression of mutant BAG3 proteins in the COS-7 cells.

The MFM patients carrying the Pro209Leu mutation were reported to demonstrate cardiac phenotypes of hypertrophic and/or restrictive cardiomyopathy, which are different from DCM. It is notable that the MFM patients manifested with cardiac phenotypes of early onset in childhood. Because the patients carrying the Arg218Trp or Leu462Pro mutations suffered from adult-onset DCM (Table 1), it was speculated that the pathological mechanisms of *BAG3* mutations might be different between the cardiomyopathy accompanied by MFM and isolated DCM. We demonstrated that the MFM-associated Pro209Leu mutation impaired the formation of multinuclear myotubes during the differentiation of C2C12 cells, which was not found with the DCM-associated mutations. However, this functional deficit may not associate with the cardiac phenotype caused by the Pro209Leu mutation, because cell fusion during the differentiation is specific to skeletal muscle cells and not found in cardiomyocytes. On the other hand, disturbance of myotube formation by the Pro209Leu mutation might be an underlying mechanism leading to skeletal muscle phenotypes in MFM, although it is not clear how the Pro209Leu mutation causes axonal neuropathy with giant axons [Odgerel et al., 2010]. Further studies will be required to reveal the difference in the molecular mechanisms of disease phenotypes caused by the *BAG3* mutations.

In conclusion, we report here two heterozygous missense mutations of *BAG3* found in familial DCM, which cause abnormal Z-disc assembly and increase the sensitivity to apoptosis in the cardiomyocytes. We demonstrate here for the first time the association between DCM and increased sensitivity to apoptosis accompanied by the abnormality in myofibrillogenesis. However, the overexpression of mutant proteins in cultured cardiac myocytes has significant limitation to mimic the situation in intact hearts. Further studies on the functional role of BAG3 protein in the cardiac muscle will help understanding the association between the abnormal function of BAG3 protein and DCM.

Acknowledgments

Conflict of Interest: None declared.

References

Arimura T, Bos JM, Sato A, Kubo T, Okamoto H, Nishi H, Harada H, Koga Y, Moulik M, Doi YL, Towbin JA, Ackerman MJ, Kimura A. 2009. Cardiac ankyrin repeat protein gene (ANKRD1) mutations in hypertrophic cardiomyopathy. J Am Coll Cardiol 54: 334–342.

Arimura T, Hayashi T, Kimura A. 2007. Molecular etiology of idiopathic cardiomyopathy. Acta Myol 26: 153–158.

Chao W, Shen Y, Zhu X, Zhao H, Novikov M, Schmidt U, Rosenzweig A. 2005. Lipopolysaccharide improves cardiomyocyte survival and function after serum deprivation. J Biol Chem 280: 21997–22005.

Chua CC, Liu X, Gao J, Hamdy RC, Chua BH. 2006. Multiple actions of pifithrin-alpha on doxorubicin-induced apoptosis in rat myoblastic H9c2 cells. Am J Physiol Heart Circ Physiol 290: H2606–H2613.

Hayashi T, Arimura T, Itoh-Satoh M, Ueda K, Hohda S, Inagaki N, Takahashi M, Hori H, Yasunami M, Nishi H, Koga Y, Nakamura H, Matsuzaki M, Choi BY, Bae SW, You CW, Han KH, Park JE, Knoll R, Hoshijima M, Chien KR, Kimura A. 2004. Tcap gene mutations in hypertrophic cardiomyopathy and dilated cardiomyopathy. J Am Coll Cardiol 44: 2192–2201.

Hishiya A, Kitazawa T, Takayama S. 2010. BAG3 and Hsc70 interact with actin capping protein CapZ to maintain myofibrillar integrity under mechanical stress. Circ Res 107: 1220–1231.

Hishiya A, Salman MN, Carra S, Kampinga HH, Takayama S. 2011. BAG3 directly interacts with mutated alphaB-Crystallin to suppress its aggregation and toxicity. PLoS One 6: e16828.

Homma S, Iwasaki M, Shelton GD, Engvall E, Reed JC, Takayama S. 2006. BAG3 deficiency results in fulminant myopathy and early lethality. Am J Pathol 169: 761–773.

Inagaki N, Hayashi T, Arimura T, Koga Y, Takahashi M, Shibata H, Teraoka K, Chikamori T, Yamashina A, Kimura A. 2006. Alpha B-crystallin mutation in dilated cardiomyopathy. Biochem Biophys Res Commun 342: 379–386.

Kimura A. 2010. Molecular basis of hereditary cardiomyopathy: abnormalities in calcium sensitivity, stretch response, stress response and beyond. J Hum Genet 55: 81–90.

Lee H, Cherk S, Chan S, Wong S, Tong T, Ho W, Chan A, Lee K, Mak C. 2011. BAG3-related myofibrillar myopathy in a Chinese family. Clin Genet, doi: 10.1111/j.1399-0004.2011.01659.x. [Epub ahead of print]

Lee JH, Takahashi T, Yasuhara N, Inazawa J, Kamada S, Tsujimoto Y. 1999. Bis, a Bcl-2-binding protein that synergizes with Bcl-2 in preventing cell death. Oncogene 18: 6183–6190.

Maron BJ, Towbin JA, Thiene G, Antzelevitch C, Corrado D, Arnett D, Moss AJ, Seidman CE, Young JB. 2006. Contemporary definitions and classification of the cardiomyopathies: an American Heart Association Scientific Statement from the Council on Clinical Cardiology, Heart Failure and Transplantation Committee; Quality of Care and Outcomes Research and Functional Genomics and Translational Biology Interdisciplinary Working Groups; and Council on Epidemiology and Prevention. Circulation 113: 1807–1816.

Murata S, Chiba T, Tanaka K. 2003. CHIP: a quality-control E3 ligase collaborating with molecular chaperones. Int J Biochem Cell Biol 35: 572–578.

Naito AT, Okada S, Minamino T, Iwanaga K, Liu ML, Sumida T, Nomura S, Sahara N, Mizoroki T, Takashima A, Akazawa H, Nagai T, Shiojima I, Komuro I. 2010. Promotion of CHIP-mediated p53 degradation protects the heart from ischemic injury. Circ Res 106: 1692–1702.

Norton N, Li D, Rieder MJ, Siegfried JD, Rampersaud E, Zuchner S, Mangos S, Gonzalez-Quintana J, Wang L, McGee S, Reiser J, Martin E, Nickerson DA, Hershberger RE. 2011. Genome-wide studies of copy number variation and exome sequencing identify rare variants in BAG3 as a cause of dilated cardiomyopathy. Am J Hum Genet 88: 273–282.

Odgerel Z, Sarkozy A, Lee HS, McKenna C, Rankin J, Straub V, Lochmüller H, Paola F, D'Amico A, Bertini E, Bushby K, Goldfarb LG. 2010. Inheritance patterns and phenotypic features of myofibrillar myopathy associated with a BAG3 mutation. Neuromuscul Disord 20: 438–442.

Pratt WB, Morishima Y, Peng HM, Osawa Y. 2010. Proposal for a role of the Hsp90/Hsp70-based chaperone machinery in making triage decisions when proteins undergo oxidative and toxic damage. Exp Biol Med 235: 278–289.

Selcen D, Muntoni F, Burton BK, Pegoraro E, Sewry C, Bite AV, Engel AG. 2009. Mutation in BAG3 causes severe dominant childhood muscular dystrophy. Ann Neurol 65: 83–89.

Takayama S, Xie Z, Reed JC. 1999. An evolutionarily conserved family of Hsp70/Hsc70 molecular chaperone regulators. J Biol Chem 274: 781–786.

Villard E, Perret C, Gary F, Proust C, Dilanian G, Hengstenberg C, Ruppert V, Arbustini E, Wichter T, Germain M, Dubourg O, Tavazzi L, Aumont MC, Degroote P, Fauchier L, Trochu JN, Gibelin P, Aupetit JF, Stark K, Erdmann J, Hetzer R, Roberts AM, Barton PJ, Regitz-Zagrosek V, Aslam U, Duboscq-Bidot L, Meyborg M, Maisch B, Madeira H, Waldenstrom A, Galve E, Cleland JG, Dorent R, Roizes G, Zeller T, Blankenberg S, Goodall AH, Cook S, Tregouet DA, Tiret L, Isnard R, Komajda M, Charron P, Cambien F. A genome-wide association study identifies two loci associated with heart failure due to dilated cardiomyopathy. Eur Heart J 32: 1065–1076.